

# OBSERVATION OF SUB-THZ COHERENT RADIATION FROM THE LINAC BEAM INJECTED IN THE NEWSUBARU STORAGE RING

Y. Shoji<sup>#</sup>, NewSUBARU/SPring-8, University of Hyogo, Japan

## Abstract

Sub-THz coherent synchrotron radiation (CSR) from the SPring-8 linac beam was observed in the NewSUBARU storage ring. The beam from the linac has much shorter bunch length than the stationary stored bunch in the ring. Then the strong CSR is observed in the ring at just after the injection until the bunch becomes long by energy dilution. We have had reported that when the linac bunch is compressed at the beam transport line and the ring is quasi-isochronous, very strong CSR was emitted in the ring for a few tens of turns. However even with parameters for the daily operation, the injected linac beam is still much shorter than that stored in the ring and CSR is observable. This report explains our experience of observing CSR at the injection, which would help to understand the beam behavior at more extreme cases and a temporal production of short-pulsed beam.

## INTRODUCTION

It is known that a short electron bunch in accelerator emits strong coherent synchrotron radiation (CSR) in wavelength region of the bunch length. There have been some proposed methods to produce a short electron bunch in a storage ring. The most conventional and wellknown is the quasi-isochronous operation [1] and the CSR burst due to the instability. However in these years, some methods of temporal short bunch production or CSR emission have been proposed such as the laser-slicing method [2], the production of bunch modulation using chromaticity modulation [3] and the circulation of linac-compressed short bunch [4, 5]. In these methods, CSR producing bunch do not survive long in a ring.

The other well-known fact is the temporal CSR emission of the linac beam when it is injected into a storage ring. Commonly the injected linac bunch is short enough to emit sub-THz CSR. This scheme has similar aspects with other new ideas, the compressed linac beam injection into the quasi-isochronous ring and also the multi-turn Energy Recovery Linac (ERL). Here we report our experience of observing CSR at the injection of the SPring-8 linac beam into the NewSUBARU storage ring. We hope that our experience would help to understand the beam behavior at the extreme cases mentioned above.

We have already tried the injection of the linac-compressed bunch into the quasi-isochronous ring [4]. At that situation, the linac beam pulse had a single bunch, 6 ps FWHM, and the charge of 0.02 nC/pulse. On the other hand in the present daily operation of the SPring-8 linac, the pulse has commonly 3 bunches and 0.2 nC/pulse and still emits CSR at the injection.

<sup>#</sup>shoji@lasti.u-hyogo.ac.jp

## MEASUREMENTS

### Set-up for the Measurement

Fig. 1 shows the layout of the SPring-8 linac [6], the booster synchrotron, and the NewSUBARU storage ring (NS) [7]. Table I and Table II show the main parameters for the linac and NS. The injection scheme is a single bucket injection.

NS has six modified double bend achromat (DBA) cells with an 8° inverted bending magnet between two 34° normal bending magnets. Fig. 2 shows the layout of the injection point and the light extraction ports of NS. The port named as SR5, using Be mirror and a quartz window, was used for the measurement. It is located at the first bending magnet just after the injection point.

Table 1: Main Parameters of the Linac

Rf frequency	2856 MHz
Transverse emittance (HWHM <sup>2</sup> )	25 $\pi$ nmrad.
Electron energy	1 GeV

Table 2: Main Parameters of NewSUBARU at 1 GeV

Rf frequency	499.955 MHz
Revolution period	396 ns
Momentum compaction factor	0.00136
Natural energy spread	0.047 %
Longitudinal damping time	12 ms
Rf acceleration voltage	120 kV

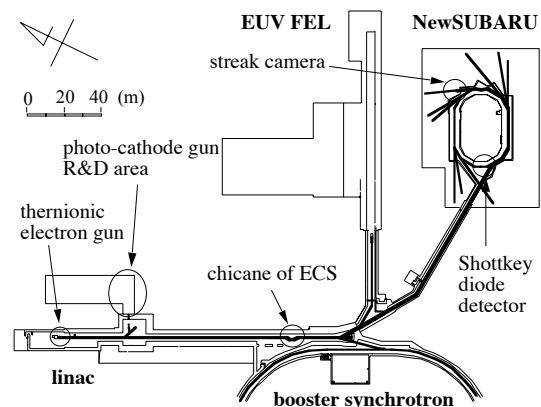


Figure 1: Layout of the SPring-8 linear accelerator (linac), the energy compression system (ECS), the booster synchrotron, and the NewSUBARU storage ring (NS).

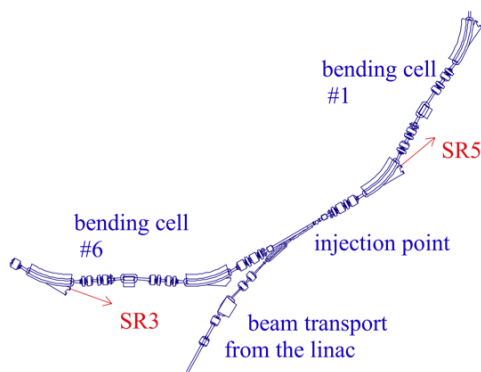


Figure 2: Layout of the Light extraction ports at NS.

**Linac Beam Measurement**

The parameters of the linac beam were measured using the double-sweep streak camera set at SR5. Fig. 3 shows the double sweep image of the injected beam with parameters of the daily operation. The time structure of the pulse at just after the injection is shown in Fig. 4. One linac beam pulse contains two strong and one weak bunches. The FWHM lengths of the front bunch and the middle bunch were 10 ps and 17 ps FWHM, respectively.

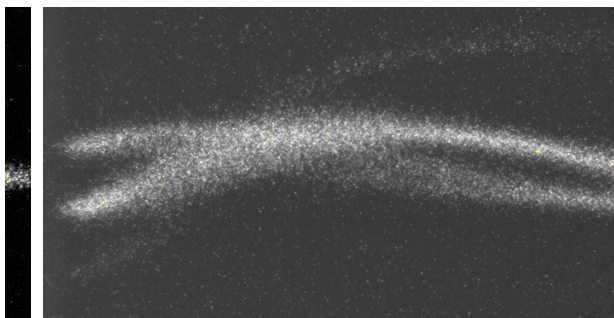


Figure 3: Synchrotron oscillation of three linac bunches injected into one storage ring rf bucket. The full ranges of the double sweep image were 2 ns in vertical (ring rf period) and 140 μs (354 revolutions) in horizontal. The narrow picture at the left shows the rf phase of the stationary stored beam. The image was multi-exposure of 10 shots.

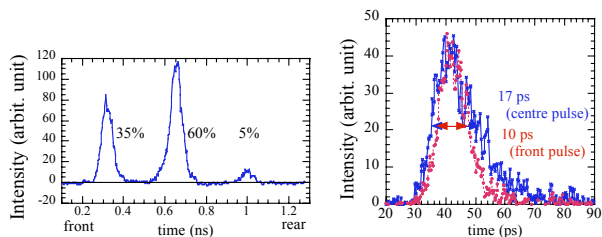


Figure 4: Time profile of one beam pulse (left) and those of the front and the middle bunch (right) at the injection.

The energy spread was estimated from the time spread after a quarter of the synchrotron oscillation period [8]. The FWHM spread was 0.4% and 0.6% for the front bunch and the middle bunch, respectively.

The beam charge was roughly 0.2 nC per pulse.

**CSR Power Measurement**

The relative CSR power was measured using two Schottky diode detectors, set side by side at the same light extraction port. One (DXP-08, Millitech Inc.) had sensitivity to a radiation of 0.09–0.14 THz and another (WR2.2ZBD, Virginia Diode Inc.) had sensitivity to 0.33–0.50 THz. The long memory oscilloscope (20Gs/s) recorded their signals for 200 μs (about 500 revolutions).

Figure 5 shows typical pulse shapes from the detectors. The most of pulses from the long wavelength detector (DXP-08) had the same shape as those of #27 and #18 of Fig. 5. Three pulses of 3 shots in 30 shots had a different shape like that of #28. Probably at these 3 shots the timing gate for the beam pulse was displaced and the pulse had a different bunch structure. The pulse from the short wavelength detector (WR2.2ZBD) had larger variation than that from DXP-08. This was because the shape was a reflection of the amplitude of microstructure in each of the three bunches.

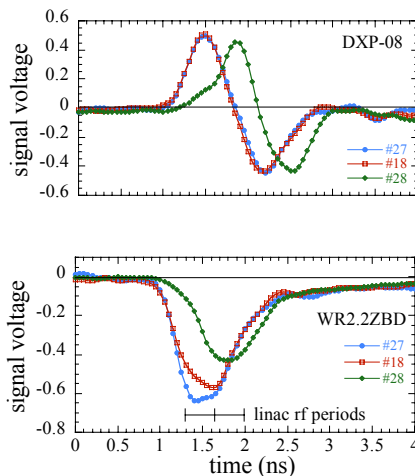


Figure 5: Typical signal shapes from the long wavelength detector DXP-08 (above) and the short wavelength detector WR2.2ZBD (below).

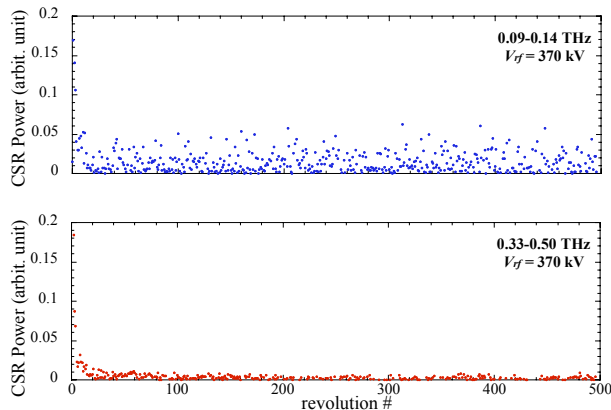


Figure 6: Typical results of turn-by-turn CSR power for one shot. The peaks after 20 turns at 0.09-0.14 THz were noise peaks.

The measurements of 10 shots took place for each of three rf acceleration voltage ( $V_{rf}$ ). For  $V_{rf}=70$  kV, 125 kV, and 370 kV, the synchrotron oscillation frequency was 4.11 kHz, 5.74 kHz, and 10.04 kHz, respectively. Fig. 6 shows typical results of the measurement, turn-by-turn CSR power. CSR power went down with revolutions and almost disappeared after 20 revolutions.

After every half of the synchrotron oscillation period, the bunch length became short again. However no CSR was detected probably because the bunch shape did not come back to the initial by a strong non-linearity of the rf bucket.

Figure 7 shows the pulse charge, measured by CT at the transport line, and the CSR power at the 1st turn. If the bunch shape were perfectly the same, the CSR power should have been proportional to the square of the pulse charge. The correlation existed, however the fluctuation of CSR power was enhanced especially for the shorter wavelength.

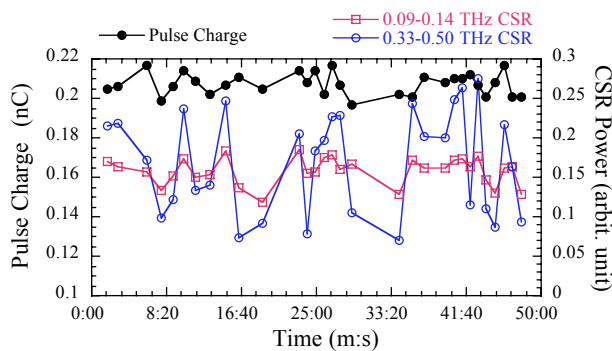


Figure 7: Injected pulse charge and CSR power at the initial turn, just after the injection.

Correlation of 0.33-0.50 THz CSR powers at the 1st and the 2nd turns had an interesting structure as shown in Fig. 8. It looked as if there were 2 groups and the data points of each group was on the line. This structure was produced by a changing pattern of 0.33-0.50 THz CSR with revolutions. Fig. 8 shows the typical patterns at the initial 12 turns. At certain turns until the 4th, the CSR power took the maximum. Only when CSR power at the 1st turn was low, we got high CSR power at the 3rd or 4th turns.

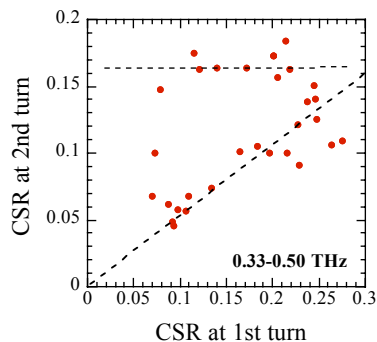


Figure 8: Correlation of CSR power at the initial (1st) turn and the next (2nd) turn.

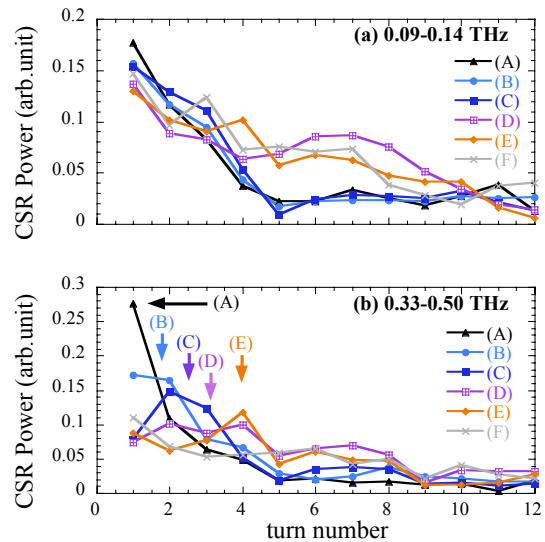


Figure 9: Typical patterns of CSR power change with revolutions from (a) the long wavelength detector DXP-08 and (b) the short wavelength detector WR2.2ZBD.

## SUMMARY AND DISCUSSION

We measured the time structure of the CSR power from the linac-produced beam in the storage ring at just after the injection. We believe that the fine time structure, which emitted short wavelength CSR, was produced before the injection. As far as we saw the CSR burst from the stored beam due to the beam instability, 0.09-0.14 THz burst starts earlier than the 0.33-0.50 THz burst by several tens turns.

The CSR at after a half of the synchrotron oscillation period was too weak to be detected. Probably because the bunch shape did not come back to the initial by a strong non-linearity of the rf bucket.

In this measurement we observed no signal much after the injection. However, we observed CSR at the different measurement using the different detector (WR3.4ZBD, 0.22-0.325 THz) at the different port (SR3 in Fig. 2), and with higher pulse charge of 0.34 nC. We will have more measurements with various conditions, for example, using an rf bucket with small non-linear terms.

## REFERENCES

- [1] M. Abo-Bakr, *et al.*, PRL. **90**, 094801 (2003).
- [2] A. Zholents, *et al.*, NIM A425 (1999) 385.
- [3] Y. Shoji, PR ST-AB 13, 060702(2010).
- [4] T. Matsubara, *et al.*, AIP CP879, 17 (2007).
- [5] H. Hama, Proc. of 27th Int. FEL Conf., p.1 (2005).
- [6] H. Hanaki, *et al.*, Proc. of 2004 APAC, pp. 3585.
- [7] A. Ando, *et al.*, *Jour. Synchrotron Radiation* **5** (1998) 342.
- [8] T. Matsubara, *et al.*, PR ST-AB 9, 042801 (2006).